

Hairpin Vortex Solution in Planar Couette Flow : A Tapestry of Knotted Vortices

著者	Itano Tomoaki, Generalis Sotos C.
journal or publication title	Physical Review Letters
volume	102
page range	114501-1-114501-4
year	2009-03
権利	Copyright (C) 2009 American Physical Society
URL	http://hdl.handle.net/10112/1283

doi: 10.1103/PhysRevLett.102.114501

Hairpin Vortex Solution in Planar Couette Flow: A Tapestry of Knotted Vortices

Tomoaki Itano

Department of Pure and Applied Physics, Faculty of Engineering Science, Kansai University, Osaka, 564-8680, Japan

Sotos C. Generalis

School of Engineering and Applied Sciences, Division of Chemical Engineering and Applied Chemistry, Aston University, United Kingdom

(Received 20 August 2008; published 19 March 2009)

A numerical continuation method has been carried out seeking solutions for two distinct flow configurations, planar Couette flow (PCF) and laterally heated flow in a vertical slot (LHF). We found that the spanwise vortex solution in LHF identifies a new solution in PCF. The vortical structure of our new solution has the shape of a hairpin observed ubiquitously in high-Reynolds-number turbulent flow, and we believe this discovery may provide the paradigm for a hierarchical organization of coherent structures in turbulent shear layers.

DOI: 10.1103/PhysRevLett.102.114501

PACS numbers: 47.27.De, 47.20.Ky, 47.27.nd

An influential study on the vortex organization in the turbulent boundary layers was recently performed by Perry & Marušić [1]. The essential finding of their study was that in the attached eddy hypothesis, in order to obtain the correct quantitative results for all components of the Reynolds stresses, two types of eddies are necessary, the “wall structure” (near-wall vortex structure attached to the wall) and the “wake structure” (vortex structure not extending to the wall). If both types are taken into account, then their theory, with data from equilibrium and quasi-equilibrium flows, can predict turbulent Reynolds stresses correctly.

Planar Couette flow (PCF) is a prototype of canonical wall-bounded shear flows, where the qualitative aspects of the fundamental structures of turbulent shear flows are tested. In PCF, a “wall structure” was first identified in Ref. [2] (see also Refs. [3–5]) as the nontrivial equilibrium state containing the streamwise vortices with spanwise wavy modulation. Moreover, the recent discovery [6] of periodic solutions rooted at the equilibrium state of PCF has stimulated many researchers [7,8] to attempt to illuminate the relevance of equilibrium states in the transition from laminar to the early stages of turbulence in this prototype flow. These equilibrium states were obtained within the framework that, before tackling a high-Reynolds-number turbulent regime, the understanding of the sustaining process in turbulent shear flows at relatively low Reynolds values should be undertaken.

At higher Reynolds numbers, another predominant structure is the hairpin vortex (horse-shoe, Λ - or Ω -shaped, attached vortex loops), which is observed to be ubiquitous in the region away from the near-wall both experimentally and numerically (for recent summary, see Ref. [9]). This structure was first envisaged by Theodorsen [10] as a “wake structure” in the boundary layer. In spite of a number of attempts since his proposition, the equilib-

rium state that corresponds to such a hairpin has never been identified so far. There is, therefore, still a controversy about the distinction between streamwise and hairpin vortices. In this Letter, we propose a way of isolating the steady hairpin vortex state in PCF by tracing a homotopy parameter. As a byproduct of our analysis, it is found that the streamwise vortex bifurcates from the hairpin vortex via a symmetry breaking in the homotopy parameter space.

In order to identify the hairpin vortex solution in PCF, we first consider an incompressible Boussinesq fluid with $Pr = 0$ filling a vertical slot of thickness $2\tilde{h}$ (see Fig. 1). The boundaries of the gap are two rigid parallel planes of infinite extent heated laterally with temperatures $\tilde{T}_0 \pm \Delta\tilde{T}$, and which move relative to each other with speed $2\Delta\tilde{U}$ in the x -direction of the Cartesian coordinate system of Fig. 1.

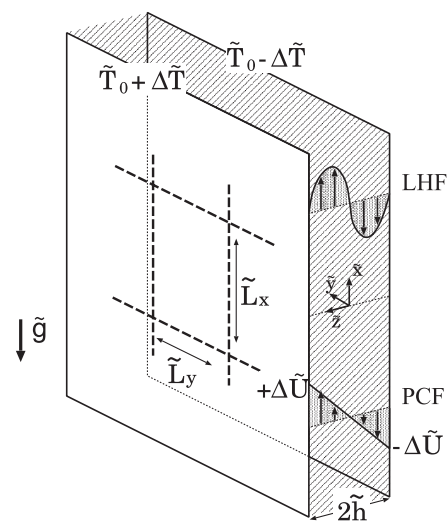


FIG. 1. Schematic view of the fluid flow in a vertical slot between laterally heated boundaries moving in the opposite directions.

Here, \tilde{T}_0 is the reference temperature. The governing equations for the perturbation, \mathbf{u} , from the laminar state of our system may be nondimensionalized uniquely in terms of two parameters, $\text{Re} = (\tilde{A} + \Delta\tilde{U})\tilde{h}/\tilde{\nu}$ and $\epsilon = \tilde{A}/(\tilde{A} + \Delta\tilde{U})$, where $\tilde{A} = \tilde{\gamma}\tilde{g}\Delta\tilde{T}\tilde{h}^2/6\tilde{\nu}$. Here, $\tilde{\gamma}$, $\tilde{\nu}$, and \tilde{g} are the coefficient of thermal expansion and kinetic viscosity at \tilde{T}_0 , and acceleration due to gravity, respectively. We impose the nonslip condition on the rigid boundaries, so $\mathbf{u}(x, y, z = \pm 1) = \pm(1 - \epsilon)\mathbf{e}_x$. The parameter ϵ plays an important role in our analysis, and we note here that solutions obtained with $\epsilon = 0$ are exact states of PCF and that those with $\epsilon = 1$ are exact states of laterally heated flow in a vertical slot (LHF).

Among the various solutions that our system might exhibit, those that are periodic in the streamwise and spanwise directions with wavelengths L_x and L_y , respectively, are of particular interest in the present study. In order to search for such standing wave solutions, we set $\partial_t = 0$ and we expand the unknown variables \mathbf{u} that uniquely determine the nature of the unknown solutions in terms of infinite Fourier—(modified) Chebyshev series satisfying the boundary conditions. A truncation scheme to the infinite set of coefficients was established so that a solution can be effectively derived. Taking into account the imposed symmetries (detailed later) as well as the continuity equation, we can deduce from a Galerkin-type projection quadratic equations for the reduced (truncated) independent set of coefficients of the series, which are subsequently determined with the aid of the iterative Newton-Raphson method.

The sequential bifurcation steps in LHF ($\epsilon = 1$) have received some attention over the last three decades (for example, see Refs. [11,12]). We briefly outline here the transition from the laminar state to the early stages of turbulence in LHF in order to aid our later discussion of the hairpin vortex structure for the PCF. Because of the fact that the basic flow in LHF possesses an inflection point, we expect the laminar flow to lose its stability with respect to infinitesimal disturbances although the Rayleigh criteria are applicable to the inviscid case in the strict sense. In this sequence, the laminar state first loses its stability to streamwise disturbances with wave number, $2\pi/L_x = \alpha = 1.345$, at $\text{Re} = 82.6$ due to Squire's theorem.

This instability initiates the supercritical bifurcation from the laminar state of the two-dimensional spanwise vortical structure (2DSV). Following a generic breakdown mechanism of two-dimensional elliptical flows [13], further increase of Re produces three-dimensional instabilities for the 2DSV in several ways, but the most preferred instability is caused by a three-dimensional subharmonic perturbation. The tertiary state that evolves naturally due to this instability consists of weakly oblique (in the x - y plane) spanwise vortical knots. This state satisfies the following three independent symmetries: Symmetry (\mathcal{A}) Streamwise translational and spanwise reflectional symmetry,

$[u_x, u_y, u_z]^T(x, y, z) = [u_x, -u_y, u_z]^T(x + L_x/2, -y, z)$. Symmetry (\mathcal{B}) Parity symmetry with respect to $(x, y, z) = (L_x/4, L_y/4, 0)$, $[u_x, u_y, u_z]^T(L_x/4 + x, L_y/4 + y, z) = [-u_x, -u_y, -u_z]^T(L_x/4 - x, L_y/4 - y, -z)$. Symmetry (\mathcal{C}) Parity symmetry with respect to the origin, $[u_x, u_y, u_z]^T(x, y, z) = [-u_x, -u_y, -u_z]^T(-x, -y, -z)$.

Using the states obtained at $\epsilon = 1$ as seeds, we have investigated the behavior of these states as ϵ changes from pure LHF ($\epsilon = 1$) to pure PCF ($\epsilon = 0$) by exploiting the homotopy. One might expect that the 2DSV that bifurcates from the laminar state with $\epsilon = 1$ intersects the $\epsilon = 0$ plane for larger Re , even if the laminar state of PCF contains no inflection point. However, our investigations show that the bifurcation curve for 2DSV acquires a turning point as ϵ decreases and does not reach the pure PCF limit (with $\epsilon = 0$). This result seems to be consistent with a conclusion from recent quests for two-dimensional states in PCF [14,15]. On the other hand, the aforementioned tertiary branch in LHF with $\epsilon = 1$ intersects the $\epsilon = 0$ plane. This new state in PCF ($\epsilon = 0$) has never been identified before.

In Fig. 2, the mean shear rate at the boundary, τ , is adopted as an order parameter to characterize the states in PCF ($\epsilon = 0$). Our new state, which is termed as HVS (hairpin vortex state) in the figure, has a turning point at $\text{Re} \approx 174$, and the lower branch is likely to asymptote to the laminar state. It exists even at $\text{Re} \approx 139$ for the streamwise and spanwise wave numbers $(\alpha, \beta) = (0.75, 1.37)$. For better comparison, we additionally plotted another state in PCF (we used the acronym "NBW" formed from Nagata, Busse, and Waleffe), which was found in previous studies [2–5]. According to Waleffe [5], the critical Reynolds number of NBW is $\text{Re}_c = 127.705$ at $(\alpha, \beta) = (0.577, 1.150)$.

We depict the new state in Figs. 3(a)–3(c), whereas NBW is given in Figs. 3(d)–3(f). The hairpin structure depicted as a bundle of vortex lines is observed ubiquitously in turbulent shear flows. As seen in the figures, the

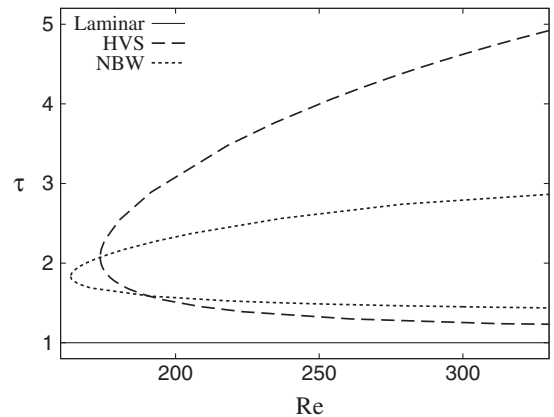


FIG. 2. Bifurcation diagram of PCF ($\epsilon = 0$) at $(\alpha, \beta) = (1, 2)$ in Re - τ plane.

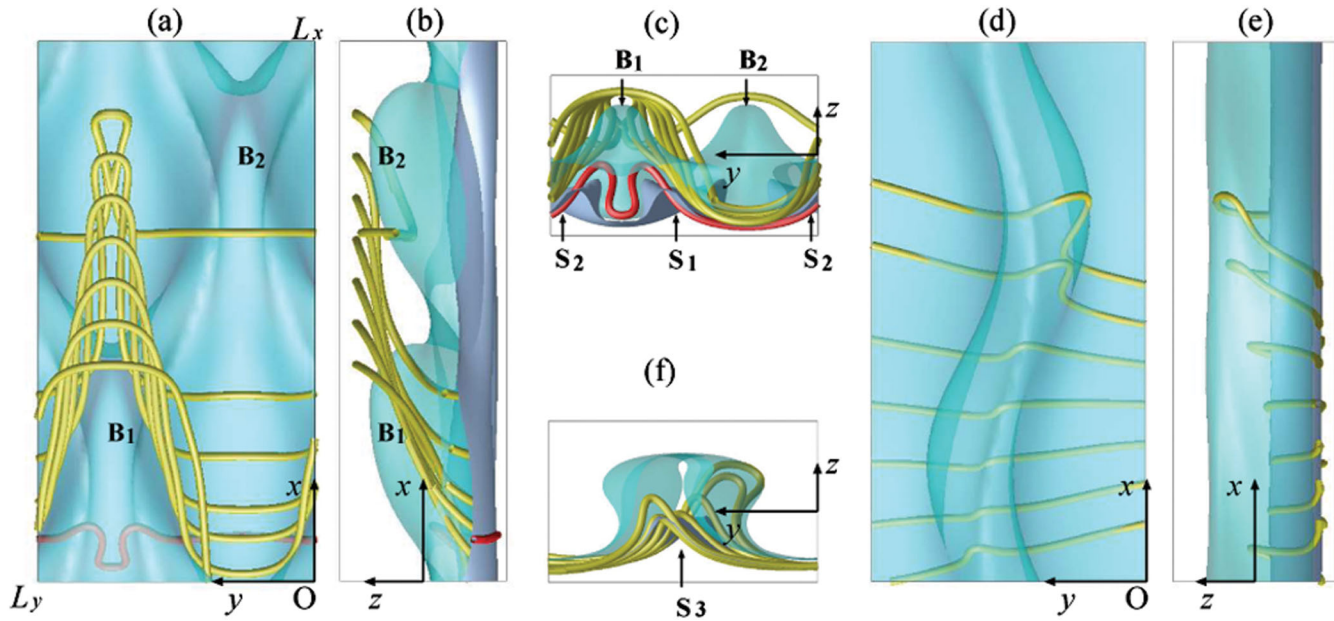


FIG. 3 (color). (a), (b), (c) The x - y , x - z , and y - z projections of the new state (upper branch) at $Re = 200$ in PCF. Yellow curves are vortex lines across the channel midplane (visualized over B_1 , but not over B_2), underneath which there are low-speed structures visualized as isosurfaces of $u_x = -0.1$ and -0.4 , colored by cyan [$z \approx \frac{1}{2}$ for the peaks of (B_1, B_2)] and blue [$z \approx -\frac{1}{2}$ for (S_1, S_2)], respectively. (d), (e), (f) Correspond to the same projections but for the upper branch of the NBW state. The vortex lines are integrated from the equivalent points located at $|z| = 0.8$ for both HVS and NBW.

most distinct difference between the new state described in this note and NBW is in their symmetry. The spanwise reflection symmetry with respect to $y = L_y/4$ (or $y = 3L_y/4$) [16] is satisfied by the former but not by the latter. NBW satisfies only two symmetries, \mathcal{A} and \mathcal{B} , so that the spanwise reflection symmetry has been broken. This moreover implies that NBW bifurcates from the LHF tertiary state via the symmetry breaking in the Re - ϵ plane, which was confirmed numerically in the present study, to take place, for example, at $Re \approx 180$ for $(\alpha, \beta) = (1, 2)$, amongst various other values. In other words, NBW is the quaternary branch, while our state is the tertiary branch in the bifurcation sequence for the laminar state. Note that NBW may exist at lower Re in PCF than our state does (see Fig. 2) because the bifurcation occurs at $\epsilon \neq 0$.

We now turn our attention to the structural flow pattern of the new state and its association to Theodorsen's wake structure of Ref. [10]. The localized vorticity lifts up the low-speed momentum fluid near the boundary ($z = -1$) so as to form *low-speed regions*, as if a tapestry of knots is intertwined with vortex lines. In NBW, such low-speed regions are formed only under where vortex lines elevate in y - z plane, as indicated as S_3 in Fig. 3(f). The elevation is produced by streamwise vorticity localized besides the low-speed region, but the three-dimensionality of the region is relatively weak in NBW [Figs. 3(d) and 3(e)], so that this region has been often referred to as *wall streak* [17] (streaky pattern aligned in x direction). Compared to NBW, the new state is intrinsically more complicated in

spite of more symmetry restrictions and consists of double structures of low-speed regions [Fig. 3(a)–3(c)]. One of them, which exists closer to the boundary than the other, is indicated by (S_1, S_2) and is visualized as bulges of $u_x = -0.4$ (blue) isosurface. The structure is streaky and similar to that appearing in NBW. The other visualized by $u_x = -0.1$ (cyan) isosurface, which exists across the midplane of the channel, is knotted rather than streaky, and shows a staggered pattern of intertwined knots of low-speed regions in the x - y plane (the bulges observed at B_1 and B_2). The former (S_1, S_2) is attributed to the near-wall vortex line with two hairpin kinks (described by a red curve in the figures), while the latter (B_1, B_2) is related to the bundle of (yellow) vortex lines with a single hairpin kink.

While HVS is kept static, as its monotonic predecessor in LHF, under the dynamical interaction between upper and lower boundaries, vortex lines (material line elements) are advected by the flow. Following the upflow from the boundary, the near-wall vortex line with two hairpin kinks may develop into a vortex line with a single hairpin kink over the channel midplane. Such a growth of the number of hairpin kinks with distance from the boundary was suggested in Ref. [9] as a possible vortex reconnection event, where the legs of multiple hairpins near the boundary realign and connect so as to form a wider hairpin. The double structural flow pattern in the new state would account for the fact that the mean shear rate of the upper branch of the new state is larger than that of NBW (see Fig. 2). This fact is also reflected in the several subtle

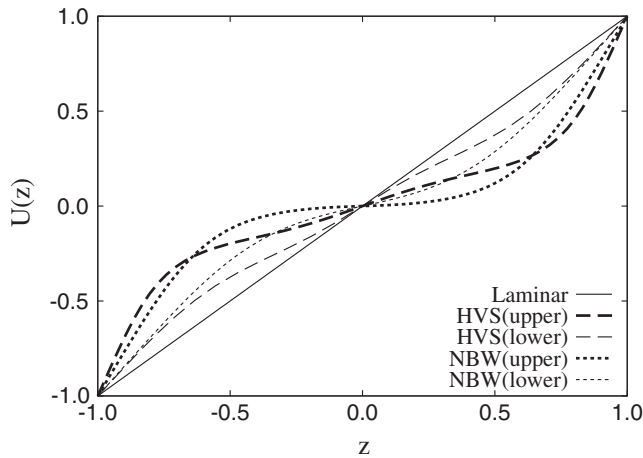


FIG. 4. Mean velocity profile of NBW and the new state (HVS) in PCF at $Re = 200$.

inflection points seen in the mean velocity profile for the upper branch of the HVS (Fig. 4). The knots of the hairpin structure are responsible for the higher stress value and would account for the predominance of the HVS at higher Reynolds numbers.

The spatial allocation of hairpin vortices and low-speed bulges on the x - y projection [Fig. 3(a)] is even reminiscent of the peak-valley pattern of Λ -shaped vortices staggered in the “Herbert style,” which was observed in experiments of turbulent transition in boundary layers [18]. The previous theoretical quests for three-dimensional nonequilibrium state in the transition stages were mostly based on the linear or weak-nonlinear analysis of the two-dimensional state under the Floquet assumption. Thus, attention has always been focused on the search for a nonlinear two-dimensional equilibrium state in PCF that would provide the route for identifying a new, alternative, three-dimensional state in PCF. Strictly two-dimensional steady solutions of PCF, for example, were the subject of investigation in Refs. [14,15], where the authors reported that they were unable to obtain such solutions, albeit limited in their simulative efforts by the necessary grid representation of the wall normal coordinate.

We may describe the results of previous literature and discuss our results in relation to them as follows. It has been established both numerically and experimentally that hairpin vortices, or stretched vortex loops or vortex pairs, are a major constituent of the turbulent shear flows for a wide range of Reynolds numbers. Furthermore, it appears that these hairpin vortices are a structure with a substantial presence over the entire region of the channel for the Reynolds number values examined. It has been remarked in the literature that a wide variation in the spanwise scales of hairpins might be expected in the wall region although it

is not clear how these vortices would reconnect and produce the long streaks apparent in the turbulent regime [19].

Here, instead of attempting to establish a homotopy between a noninflectional flow and Couette flow, we chose to include a shear flow with an inflection point in order to establish a route via which a *new solution* to the Couette flow can be found. Although the obtained state is the more primitive branch from which the equilibrium state previously obtained in PCF is bifurcated, it has a richer vortex structure and may even provide an exact expression for an equilibrium state of a possible vortex reconnection event in the near-wall region. The present results may shed some light on the historical debate concerning the roles of streamwise and hairpin vortices in turbulent flow.

T. I. is grateful for the financial support received from Aston University under the Visiting Scholars Fund Scheme and EPSRC (GR/S70593/01), which allowed him to spend time in the United Kingdom, while working on this project. S. C. G. is grateful for a Research Invitation from the Kansai University, which allowed him to spend time in Japan during the final stages of this work. This work has been also supported in part by KAKENHI (19760123).

-
- [1] A. E. Perry and I. Marusic, *J. Fluid Mech.* **298**, 361 (1995).
 - [2] M. Nagata, *J. Fluid Mech.* **217**, 519 (1990).
 - [3] R. M. Clever and F. H. Busse, *J. Fluid Mech.* **344**, 137 (1997).
 - [4] F. Waleffe, *Phys. Rev. Lett.* **81**, 4140 (1998).
 - [5] F. Waleffe, *Phys. Fluids* **15**, 1517 (2003).
 - [6] G. Kawahara and S. Kida, *J. Fluid Mech.* **449**, 291 (2001).
 - [7] D. Viswanath, *J. Fluid Mech.* **580**, 339 (2007).
 - [8] J. F. Gibson, J. Halcrow, and P. Cvitanovic, *J. Fluid Mech.* **611**, 107 (2008).
 - [9] R. J. Adrian, *Phys. Fluids* **19**, 041301 (2007).
 - [10] T. Theodorsen, *Proc. Second Midwestern Conf. on Fluid Mechanics* (Ohio State University, Columbus, Ohio, USA, 1952), pp. 1–19.
 - [11] M. Nagata and F. Busse, *J. Fluid Mech.* **135**, 1 (1983).
 - [12] M. Nagata and T. Itano, *Proc. of Conference on Modelling Fluid Flow* (Budapest University, Budapest, Hungary, 2003), pp. 588–594.
 - [13] F. Waleffe, *Phys. Fluids A* **2**, 76 (1990).
 - [14] P. G. Mehta and T. J. Healey, *Phys. Fluids* **17**, 094108 (2005).
 - [15] F. Rincon, *Phys. Fluids* **19**, 074105 (2007).
 - [16] The spanwise reflection symmetry with respect to the $y = L_y/4$ plane, $[u_x, u_y, u_z]^T(x, L_y/4 + y, z) = [u_x, u_y, u_z]^T(x, L_y/4 - y, z)$, can be deduced by the symmetries \mathcal{A} , \mathcal{B} , and \mathcal{C} .
 - [17] S. K. Robinson, *Annu. Rev. Fluid Mech.* **23**, 601 (1991).
 - [18] T. Herbert, *Annu. Rev. Fluid Mech.* **20**, 487 (1988).
 - [19] R. J. Adrian, C. D. Meinhart, and C. D. Tomkins, *J. Fluid Mech.* **422**, 1 (2000).